ACI MATERIALS JOURNAL TECHNICAL PAPER

Title no. 110-M07

Chemo-Mechanical Micromodel for Alkali-Silica Reaction

by Wiwat Puatatsananon and Victor Saouma

This paper presents a two-stage numerical model for alkali-silica reaction (ASR)/stress analysis in concrete. The coupled analytical chemo-mechanical model developed by Suwito et al. was modified to include the effects of internal moisture and ion concentration on the transport properties of concrete. A finite difference model was used to simulate the coupled diffusion of alkali into concrete and subsequent ASR gel into pores surrounding the aggregates. A finite element model was then subsequently used to perform a nonlinear analysis. This model is invoked from the master finite difference model, resulting in a coupled chemo-mechanical simulation of ASR-affected concrete with aggregates of different shapes and sizes. Throughout this analysis, the authors keep track of the vertical and lateral expansions of the concrete with time which, in turn, are transformed into equivalent anisotropic coefficients of ASR expansion. Finally, the accuracy of the model is assessed through comparison with simulated laboratory tests.

Keywords: alkali-silica reaction; finite element; macromodel; micromodel.

INTRODUCTION

Alkali-silica reaction (ASR) is a chemical reaction between alkali cations and hydroxyl ions from concrete pore solutions and certain metastable or strained forms of silica present in aggregate particles. This chemical reaction will produce a gel that, in the presence of moisture, will swell. Hence, in a simplified manner, ASR can be described as a two-step reaction between alkalis (sodium and potassium) in concrete and silica-reactive aggregates. The first step is the chemical reaction between the reactive silica in the aggregate with the alkali present in concrete to produce alkali-silica gel

$$\underset{xSiO_2}{\text{reactive silica in aggregate}} + \underset{yNa(K)OH}{\text{alkali in concrete}} \rightarrow \underset{Na(K)_ySi_xO_zaqueous}{\text{alkali-silica gel}} \quad (1)$$

and the second is the expansion of the alkali-silica gel when it comes in contact with moisture

$$\underset{Na(K)_ySi_xO_zaqueous}{\text{alkali-silica gel}} + \underset{H_2O}{\text{moisture}} \rightarrow \underset{Na(K)_ySi_xO_z\ wH_2O}{\text{expanded alkali-silica gel}} \quad (2)$$

ASR was first identified by Stanton (1940) and since then, safeguards have been put in place to avoid/limit such nefarious reactions. Nevertheless, great concern remains as, on the one hand, engineers are confronted with a dwindling supply of adequate aggregates, and it is still not uncommon to be confronted with cement with an equivalent alkali content greater than the 0.6% limit; on the other hand, many dams built prior to the 1940s suffer from ASR (Saouma et al. 2007).

There is a very rich body of literature addressing the multiple aspects of this reaction, but only those addressing the coupled chemo-mechanical models (albeit within the representative volume element [RVE]) are relevant to this work.

To the best of the authors' knowledge, the first report of a coupled chemo-mechanical simulation of ASR was reported by Sellier et al. (1995). Although they did not explicitly model the two phases of the ASR reaction, Ulm et al. (2000) subsequently presented a model for ASR swelling formulated at the microlevel, which was applied at the structural one. A micro-mechanical model based on extended finite element modeling (XFEM) was developed by Dunant and Scrivener (2010); however, the model made no attempt to explicitly simulate the diffusion—only the resulting swelling.

Microscopic chemo-mechanical models go to the heart of the reaction, as they simulate both the diffusion and the expansion. One such model was developed by Suwito et al. (1998) and later expanded (Suwito et al. 2002). In this model, the diffusion of chemical ions from the pore solution into aggregate and the diffusion of ASR gel from the aggregate surface into the surrounding porous cement matrix are simulated. The total ASR gel is divided into two parts: 1) the gel directly deposited in the interface pores, which does not cause expansion; and 2) the gel permeated into the surrounding pores in the cement paste that generates the interface pressure and is responsible for the expansion. Interface pressure between aggregate and cement paste is also accounted for. The model is cast within the framework of the self-consistent method, and analytical solutions (albeit for spherical aggregates) are derived. Ultimately, this model provided an effective expansion coefficient in terms of aggregate fineness.

A similar model was subsequently developed by Poyet et al. (2007), where interface pressures are not explicitly accounted for; however, an isotropic damage caused by ASR expansion and the resulting swelling is quantified. This model was capable of capturing the kinetics of the reaction and was applied to a system of several aggregates. This model was subsequently refined by Multon et al. (2009).

One commonly performed test is ASTM C1260. It is an accelerated test to detect the potential of an aggregate intended for use in concrete for undergoing ASR, resulting in potentially deleterious internal expansion. A 25.4 x 25.4 x 254 mm (1 x 1 x 10 in.) mortar bar is moisture-cured for 1 day prior to demolding and then immersed in a sodium hydroxide solution for 14 days. Lengths are measured daily, and the expansion is assumed to be an indicator of the aggregate's reactivity. ASTM C1260 stipulates that an expansion of less than 0.1% should be considered innocuous.

Jin et al. (2000) investigated the feasibility of "glasscrete," where silica-rich waste glass is used as aggregate. Assess-

ACI Materials Journal, V. 110, No. 1, January-February 2013.
MS No. M-2011-289 received September 13, 2011, and reviewed under Institute publication policies. Pertinent discussion including author's closure, if any, will be published in the November-December 2013 *ACI Materials Journal* if the discussion is received by August 1, 2013.

Wiwat Puatatsananon *is an Assistant Professor in the Department of Civil Engineering at Ubon Ratchathani University, Ubon Ratchathani, Thailand. He received his BEng from Khon Kaen University, Khon Kaen, Thailand, and his MSc and PhD from the University of Colorado, Boulder, Boulder, CO.*

Victor Saouma *is a Professor of Structural Engineering at the University of Colorado, Boulder. His research interests include concrete degradation, fracture mechanics, and nonlinear analysis of dams and nuclear power plants.*

ment was made through ASTM C1260 mortar bar tests, where 10% of innocuous sand was substituted by glass particles of various sizes. Jin et al. (2000) showed that a decrease of particle size causes an increase of volume expansion and damage due to ASR up to a specific particle size (pessimum). When the particle size was reduced further, however, smaller ASR-induced expansions were observed, together with an increase in the compressive strength of the concrete.

This test was the impetus for Suwito et al.'s (2002) analytical model, which will be extended in the following and cast within a numerical framework. The proposed model will thus remove some of the original limiting assumptions, resulting in a highly nonlinear coupled formulation. The solution will be pursued numerically, coupling finite difference and finite element. The former will be used for the diffusion part, and the latter will be used for the determination of the interface pressure.

RESEARCH SIGNIFICANCE

The main contribution of this study is a fully coupled simulation of most of the phenomenons that cause ASR which, in turn, will enable researchers to perform parametric studies to assess the relative importance of various parameters. The second main contribution is the link between the micromodel and the macromodel that is the coupled numerical simulation of one reactive aggregate, which could ultimately yield the concrete expansion curve experimentally determined at the material level (Larive 1998).

ANALYTICAL MODEL

The original model of Suwito et al. (2002) encompasses the chemo-mechanical coupling of the ASR expansion process, the size distribution of aggregates, and the microstructural features of the cement paste and is limited to fully saturated concrete. The chemical part of the model includes two opposing diffusion processes that take place simultaneously:

1. Diffusion of the hydroxide and the alkali ions into aggregates, followed by the reaction of these ions with the reactive aggregate; and
2. Diffusion of the expansive ASR gel from the cement paste-aggregate interface out to the porous interfacial transition zone (ITZ). It is assumed that the volumetric expansion of concrete is initiated only when the volume of the reaction product exceeds the porous volume of the ITZ.

Diffusion models

There are three distinct diffusions. First, there is a macrodiffusion of ions from the sodium hydroxide solution in which the bar is immersed into the mortar bar itself. Then, a microdiffusion of those ions into the aggregates occurs, which is ultimately followed by another reversed microdiffusion of gel from the aggregates into the cement paste.

Macro-ion diffusion of alkali—Because the mortar bar is composed of nonreactive cement, ions from the sodium hydroxide solution must first diffuse into the specimen for a reaction to occur with the silica in the aggregates. It is assumed that the alkali ion causing the gel in the microlevel is negligible compared to the alkali ion concentration in the macrolevel. Hence, the decrease in the alkali ion concentration is neglected in the macro-ion diffusion analysis. Therefore, the macrodiffusion of alkali ions is similar to other macrodiffusion processes in concrete, such as moisture diffusion and chloride penetration, and is governed by Fick's law

$$B_{ion,macro}\frac{\partial C_{ion}}{\partial t}=\nabla(D_{ion,macro}(C_{ion})\nabla C_{ion}) \tag{3}$$

where C_{ion} is the free ion concentration of the pore solution inside the concrete; and $B_{ion,macro}$ and $D_{ion,macro}$ are the binding capacity and ion diffusivity of the concrete, respectively.

Micro-ion diffusion model of alkali—In the microlevel ion diffusion, the penetration of alkali ions from the pore solution into the aggregate is first simulated. To simplify the problem, it assumes that ASR occurs only when C_{ion} reaches a critical concentration C_{cr}. Therefore, the alkali ion causing the gel is neglected and the penetration of alkali ions into the aggregate is also governed by Fick's law

$$B_{ion}\frac{\partial C_{ion}}{\partial t}=\nabla(D_{ion}(C_{ion})\nabla C_{ion}) \tag{4}$$

where C_{ion} is the free ion concentration of the pore solution inside the aggregate; and B_{ion} and D_{ion} are the binding capacity and ion diffusivity of the aggregate, respectively.

It should be noted that this is a continuous process, and the moving front where $C_{ion} = C_{cr}$ varies with time t, as shown in Fig. 1. Hence, one can solve for the ASR depth as a radius $r_{cr}(t)$ in Eq. (4) by simply replacing C_{ion} with C_{cr}.

Although Suwito et al. (2002) assumed that D_{ion} is a constant in the linear model, the ion diffusivity actually decreases with the formation of gel (conservation of mass). Hence, one can assume a simplified linear model

$$D_{ion,micro}(t)=\left(1-b\cdot\frac{C_{gel}(t)}{C_p}\right)D^0_{ion,micro} \tag{5}$$

where C_p is the porosity of the cement paste; $C_{gel}(t)$ is gel concentration at the boundary of the aggregate; and b is a reduction parameter of $D_{ion,micro}$ for the saturated state of gel ($0 < b < 1$) and $b = 0.5$. As a result of the dependence of D_{ion} on the ion concentration, Eq. (4) becomes a nonlinear equation requiring a numerical solution. It should be noted that the proposed model does not account for the alkali-calcium substitution, as reported in Glasser and Kataoka (1981); this substitution may not manifest itself in accelerated laboratory tests but, rather, in the long-term swelling of dams.

For a spherical aggregate, the volume of the reacted aggregate of size R_i is given by

$$V_{R_i}(t)=\left[\frac{R_i^3-(R_i-r_{cr}(t))^3}{R_i^3}\right]\left(\frac{4}{3}\pi R_i^3\right)=\left[1-\left(1-\frac{r_{cr}(t)}{R_i}\right)^3\right]\left(\frac{4}{3}\pi R_i^3\right) \tag{6}$$

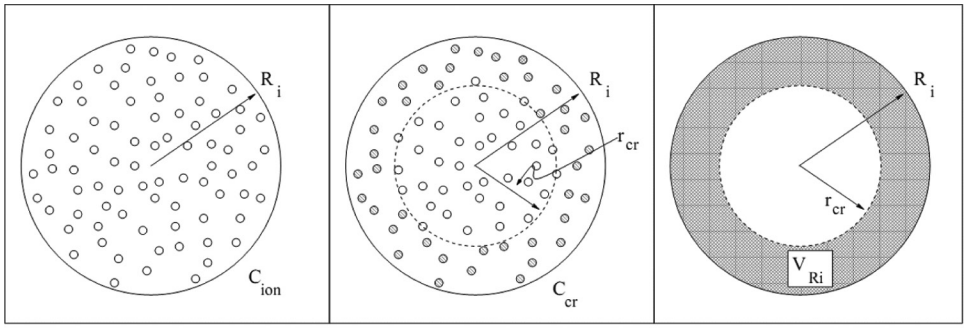

Fig. 1—Ion diffusion into aggregate.

from which we can determine the volume of the ASR gel using

$$V_{gel}^{R_i}(t) = \eta V_{R_i}(t) \tag{7}$$

where η is the volume ratio of the ASR gel to the reacted aggregate; $\eta > 1$ means that the volume of the reaction product is larger than the original volume of the aggregate, leading to volume expansion of concrete. The variable η depends on many factors, such as the type of aggregate and relative humidity H. This last dependency was quantified by Poole (Swamy 1992), who stipulated that ASR can only be activated when H is approximately 75% or higher. Thus, one can assume a bilinear dependency of η on H

$$\eta = \begin{cases} 0 & H < 50 \\ \dfrac{H-50}{50}.20\eta_0 & 50 \le H \le 82 \\ \dfrac{H-82}{18}1.\eta_0 & 82 \le H \le 100 \end{cases} \tag{8}$$

where η_0 is the volume ratio when $H = 100\%$; η_0 is taken as 1.75 in this study.

Therefore, the volume of gel outside the original boundary of the aggregate will simply be given by

$$V_{gel}^{*R_i}(t) = V_{gel}^{R_i}(t) - V_{R_i}(t) = (\eta - 1)V_{R_i}(t) \tag{9}$$

Microdiffusion of gel—At the microlevel, ASR gel accumulates along the interface zone first. Because the porosity of the interface zone can only absorb a finite volume of gel before it is saturated, any additional gel will generate an interface pressure. The effective additional volume of gel $V_{gel,eff}^{R_i}(t)$ can be determined from

$$V_{gel,eff}^{R_i}(t) = V_{gel}^{*R_i}(t) - V_{pore}^{R_i} \tag{10}$$

where $V_{gel}^{*R_i}$ is the total gel generated outside the original boundary of aggregate in the previous process; and $V_{pore}^{R_i}$ is the total volume of the pores around the reacted aggregate i (interface zone), which is given by

$$V_{pore}^{R_i} = V_{unit} A_{agg}^{Ri} \tag{11}$$

where V_{unit} is a material constant (in length scale) representing the capacity of the interface zone to absorb ASR gel per unit area; and A^{Ri}_{agg} is the surface area of an aggregate particle of size R_i. When $V_{gel,eff}^{R_i}(t)$ becomes positive, the interfacial pressure initiates and drives the gel diffusion through the porous cement paste (Fig. 2).

The ASR gel diffusion through the porous cement paste can be characterized by Darcy's law for a viscous flow as

$$\frac{\partial C_{gel}(t)}{\partial t} = \nabla\left(\frac{K_{gel}}{\eta_{gel}}\nabla P_{gel}(t)\right) \tag{12}$$

where $C_{gel}(t)$ is the concentration of the gel; and K_{gel} and η_{gel} are the gel permeability of the porous cement paste and viscosity of the gel, respectively. In this study, both K_{gel} and η_{gel} are assumed to be constant. The variable $P_{gel}(t)$ is the interface pressure distribution due to ASR gel and thus depends on the degree of saturation of the pores. At the boundary of the aggregate, the interface pressure around the aggregate due to the ASR gel, $P_{\text{int}}(t)$, is applied.

This is a coupled chemo-mechanical equation, and its solution hinges on a relationship between the pressure $P_{gel}(t)$ and the gel concentration $C_{gel}(t)$. For the ITZ (neglecting diffusion of the gel into the cement paste), such an equation was originally assumed by Suwito et al. (2002) as

$$C_{gel}(t) = \beta P_{gel}(t) \tag{13}$$

where β is the state function for the cement paste. When the pores of the cement paste are saturated with ASR gel, $C_{gel} = C_p$, where C_p is the porosity of the cement paste. Concurrently, the pressure P_{gel} reaches the saturation pressure, which can be approximated to the concrete tensile strength f_t'. Therefore, $\beta = C_p/f_t'$. Once the interface pressure due to the

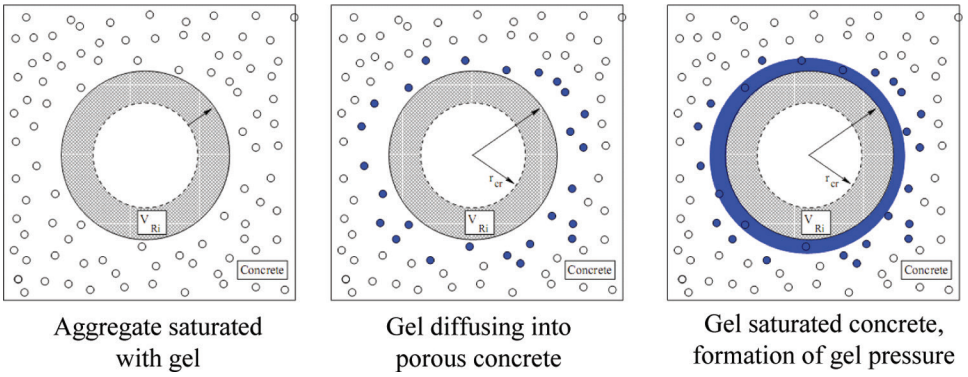

Fig. 2—Gel diffusion into cement paste.

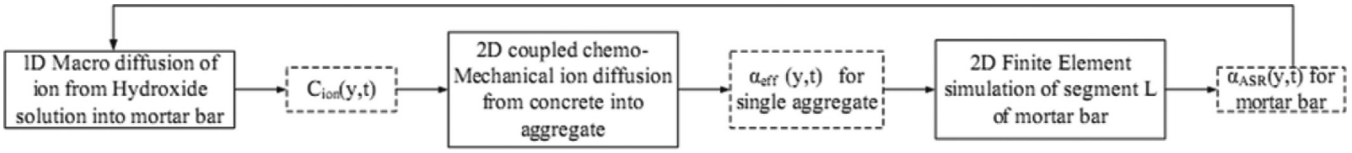

Fig. 3—Numerical procedure for ASR expansion.

ASR gel around the aggregate, $P_{\text{int}}(t)$, is determined through the stress analysis, the gel concentration at the boundary of the aggregate is determined from $C_{gel}(t) = \beta P_{\text{int}}(t)$. Hence, Eq. (12) can be expressed in terms of C_{gel} and can be solved numerically. It should be noted that Eq. (13) assumes that the gel absorbed by the cement paste is neglected, which may result in an artificially increased interface pressure between the aggregate and the cement paste because its concentration is overestimated. An alternate equation for the pressure induced by the gel is given by Sellier et al. (1995).

The total volume change due to ASR in all of the aggregates with size R_i is equal to the volume of ASR gel beyond the accommodating capacity of their interface zone. This can be expressed as $\Delta V_{gel}^{R_i}(t) = V_{gel,eff}^{R_i}(t) - V_{pg}(t)$, where $V_{pg}(t)$ is the total gel that permeated into the cement paste and $\Delta V_{gel}^{R_i}(t)$ will cause the transient internal pressure between the aggregate and the cement paste matrix, $P_{\text{int}}(t)$.

The gel volume in the porous cement paste surrounding the aggregate at time t, $V_{pg}^{R_i}(t)$, is given by

$$V_{pg}^{R_i}(t) = \begin{cases} \int_{R_i}^{R_\infty} 4\pi r^2 C_{gel}(r,t)dr & \text{3-D spherical particle} \\ \int_{R_i}^{R_\infty} 2\pi r C_{gel}(r,t)dr & \text{2-D cylindrical particle} \end{cases} \quad (14)$$

where C_{gel} is the total concentration of gel (solution of Eq. (12)). This will have to be determined either analytically or numerically.

Then, the coefficient of ASR expansion for an aggregate with radius R_i can be determined from

$$\alpha_i^{R_i}(t) = \frac{\Delta V_{gel}^{R_i}(t)}{V_a^{R_i}} = \frac{V_{gel,eff}^{R_i}(t) - V_{pg}^{R_i}(t)}{V_a^{R_i}} = \frac{V_{gel}^{*R_i}(t) - V_{pore}^{R_i} - V_{pg}^{R_i}(t)}{V_a^{R_i}} \quad (15)$$

where $V_a^{R_i}$ is the volume of aggregate with radius R_i. This equation assumes that the swelling of the aggregate is caused only by the formation of the gel outside the interface zone (the gel inside the pores does not cause swelling). Given $\Delta V_{gel}^{R_i}(t)$, $P_{\text{int}}(t)$ can be solved from the equilibrium of the composite system, which is a mechanics problem for interface stress analysis in either a three-dimensional (3-D) spherical system or a two-dimensional (2-D) cylindrical system.

Finally, the total coefficient of expansion of an ASR-affected concrete is the sum of all individual aggregate expansions (each one depending on its size). The interface pressure determined this way must be equal to the pressure obtained from the state equation used in Eq. (12). This is clearly a nonlinear formulation that can only be solved iteratively.

NUMERICAL MODEL

The previously described analytical model—an extension of the one of Suwito et al. (2002)—can only be solved numerically, as it entails the solution of coupled nonlinear equations. This will be achieved through three distinct steps: 1) macro-ion diffusion analysis; 2) micro-coupled chemo-mechanical gel diffusion analysis; and 3) macro stress analysis to determine mortar bar expansion (Fig. 3).

Furthermore, because a numerical solution is used, there is no longer the constraint of a "circular" aggregate.

Macro-ion diffusion analysis

The diffusion analysis of the ions from the concrete boundary into the concrete is performed through a finite difference scheme by using the heat transfer analysis code concrete deterioration analysis program (CDAP) (Puatatsananon 2002). This macro-ion diffusion analysis is not coupled with the micro-ion diffusion analysis because there is no term of alkali ion concentration consumed by the reaction to create gel in Eq. (3). The temporal and spatial variation of the free ion concentration is recorded for subsequent micro-ion diffusion analysis.

Micro-coupled chemo-mechanical analysis

Analysis is driven by a specially written C++ code (Puatatsananon 2002) (SIMulation of Silica Aggregate Reactions [SIMSAR]). Equations (4) and (12) are solved by a finite difference scheme. The code is coupled with a nonlinear finite element code (Saouma 2010) for the stress analysis to determine the interface pressure between the aggregate and the cement paste matrix $P_{\text{int}}(t)$; the analysis is performed only for the RVE of concrete, which has the reactive aggregate inside. The gel concentration at the boundary of the reactive aggregate is then determined from $C_{gel}(t) = \beta P_{\text{int}}(t)$ and Eq. (12) can then be solved numerically by a finite difference scheme.

The numerical simulation at a given time step t of the ion diffusion from the sodium hydroxide solution can be described as follows:

1. Initialization prior to the analysis:

- A topological representation of the aggregates (identified by the subscript i) and cement paste is first defined, and then a corresponding finite difference grid is set up.
- Initial data are critical ion concentration C_{cr}, porosity C_p, ion permeability of the aggregate $D^0_{ion,micro}$, ion binding capacity B_{ion}, and volume ratio of the ASR gel to the reacted aggregate η.

2. Micro-ion diffusion—For each time step:

- Solve for the ion diffusion into the aggregate (Eq. (4)).
- For each node, update $D_{ion}(t)$ (Eq. (5)).
- For each aggregate i:
  - Count the number of cells with $C_{ion} \geq C_{cr}$ and determine the volume of reacted aggregate $V_{R_i}(t)$.
  - Determine $V^{R_i}_{gel}(t)$ from Eq. (7) and $V^{R_i}_{gel,eff}(t)$ from Eq. (10).
  - If $V^{R_i}_{gel,eff}(t) > 0$, set $t_{gstart} = t$; then, go to the next step; otherwise, increase time step Δt and repeat ion diffusion simulation.

3. Gel diffusion with $t_{total} = t_{gstart} - t_{istart}$, $t_{gel} = t_{istart}$, and $\Delta t_{gel} = \Delta t$. Assuming $V_{pg} = 0$ and for $t_{gel} = t_{gel} + \Delta t_{gel}$, and for each time increment:

- Determine total expansion coefficient for each aggregate α^{Ri}_T from time $t = t_{istart}$ to $t = t_{gstart}$ from Eq. (15).
- Determine expansion coefficient for each time increment Δt_{gel} of gel diffusion $\alpha^{Ri}_{inc} = (t_{gel} - t_{istart})\alpha^{Ri}_T / t_{total}$.
- Pass α^{Ri}_{inc} for all of the aggregates to MERLIN (Saouma et al. 2010) for stress analysis.
- MERLIN will perform the interface stress analysis by a pseudo thermal analysis. It should be noted that given the propensity for microcracks around the aggregates due to localized high pressure, the stress analysis is nonlinear with a fracture-plasticity constitutive model (Červenka and Papanikolaou 2008).
  - Apply α^{Ri}_{inc} as $\alpha^{Ri}_{inc} = \alpha^T_i \Delta T$, where ΔT is a unit virtual temperature change for the aggregates and α^T_i will be the pseudo coefficient of thermal expansion for each particle.
  - Analyze the problem.
  - Return the traction distribution around each aggregate.
  - Return the vertical and lateral displacements.
- From the traction distribution around each aggregate, determine interface pressure. The gel concentration at the boundary of the aggregate is then determined from $C_{gel}(t) = \beta P_{\text{int}}(t)$. Note that only the interface pressure between the aggregate and cement paste is determined.
- For gel diffusion into the cement paste, solve Eq. (12) and (13).
- Count the number of nodes with nonzero gel concentration and determine the volume of gel in the porous cement at time t_n in the vicinity of particle i, $V^{R_i}_{pg}(t)$ essentially solving Eq. (14)).
- Solve for

$$\alpha^{R_i}_i = \alpha^{Ri}_{inc} - \frac{V_{pg}}{V_a}$$

- Compare α^{Ri}_i with α^{Ri}_{inc}. If their difference is within the prescribed tolerance, increase the time step in the gel diffusion and perform the analysis in the next increment of the gel diffusion; otherwise, store the value of $\alpha^{Ri}_{inc} = \alpha^{Ri}_i$, then pass α^{Ri}_{inc} back to MERLIN until convergence.
- If $t_{gel} = t_{gstart}$, determine the isotropic or anisotropic (if the RVE has different confining tractions in the vertical and horizontal directions) ASR-induced strain

$$\varepsilon^{ASR}_x(t) = \frac{u_x}{\text{width}} \tag{16}$$

$$\varepsilon^{ASR}_y(t) = \frac{u_y}{\text{height}} \tag{17}$$

record the bigger value of the two strains as the expansion coefficient due to the ASR gel in that RVE ($\alpha_{RVE}(t)$); then, increase time step t and go back to analyze for the ion diffusion. The anisotropic loading is not assumed to change gel pressure.

The algorithm for the coupled chemo-mechanical simulation of the gel diffusion into the aggregate is shown in Fig. 4. In summary, the major differences between the original analytical model of Suwito et al. (2002) and the proposed numerical model are:

1. The numerical model can handle multiple and nonspherical aggregates.

2. The interface pressure distribution is more accurately determined through a nonlinear finite element analysis.

3. The effects of humidity and ion concentration are accounted for through Eq. (5) and (8).

Macro stress analysis

Once the expansion of an aggregate has been determined in terms of elevation y and time t, the overall bar expansion is sought next. A macro finite element mesh, in which one in 10 aggregates' location is assumed to be reactive, is prepared. At each time step, the expansion is provided from the previous analysis and a stress analysis is performed with MERLIN. For simplification, the problem formulation exhibits only a one-way coupling, and the stress state assessed in the macro stress analysis is not accounted for at the REV level. Furthermore, the gel cannot permeate outside the boundary of the REV in the micro gel diffusion analysis. This, in turn, will provide the overall mortar bar expansion in terms of time.

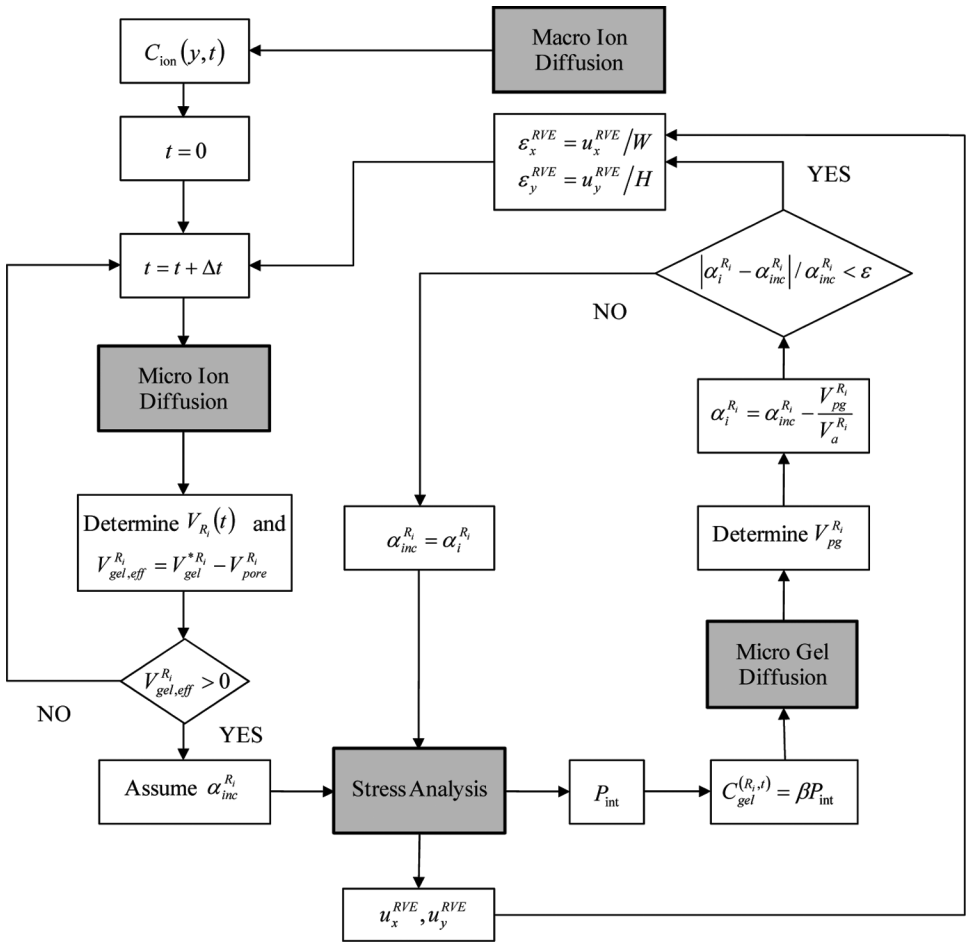

Fig. 4—Algorithm of coupled simulation of SIMSAR and MERLIN.

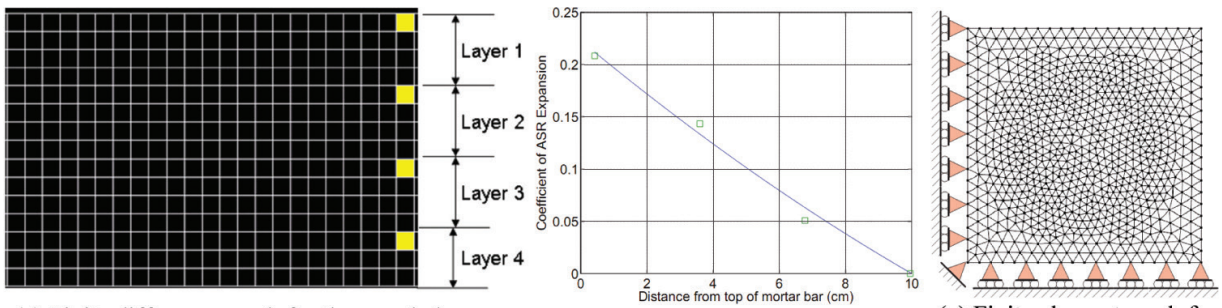

(a) Finite difference mesh for the coupled macro-analysis

(b) Linear regression for ASR expansion in terms of depth

(c) Finite element mesh for a single aggregate RVE

Fig. 5—Numerical discretizations.

EXAMPLE

Model

The initial macro diffusion of ions from the external hydroxide solution into the concrete (Eq. (3)) was performed through pseudo one-dimensional (1-D) finite difference analysis with 31 nodes across and 31 vertical. The subsequent RVE for the coupled chemo-mechanical model required a total of three meshes. The finite difference mesh for micro-ion diffusion of one single aggregate (thus ignoring interaction among adjacent aggregates in this step) was fixed at 620 by 620. The finite element mesh for single aggregate stress analysis is shown in Fig. 5(c); the same generic mesh was used for all aggregate sizes by simply scaling the dimensions.

The finite element mesh for macro analysis from which global response is sought is shown in Fig. 6. Given the variation of aggregate sizes, only a representative segment L of the mortar was modeled for stress analysis (Fig. 6(a)). Table 1 shows L and the number of elements in the vertical direction for each one of the meshes (they all had a height equal to 12.7 mm [0.5 in.], which corresponds to half the height of the mortar bar). The REV size used in the micro-

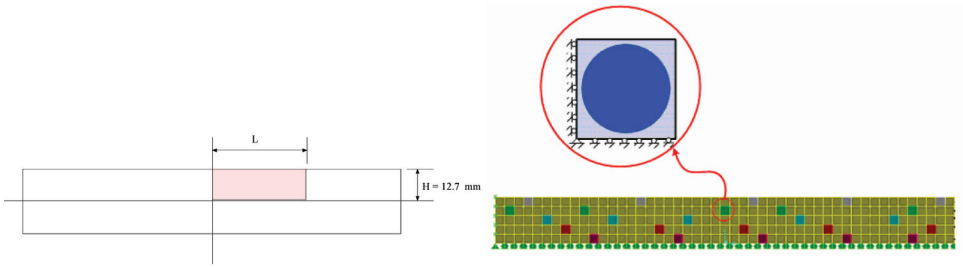

(a) Modelled segment of the mortar bar

(b) Corresponding finite element mesh for stress analysis, and RVE for the micro diffusion

Fig. 6—Mortar bar simulation. (Note: 1 mm = 0.03937 in.)

Fig. 7—Free ion concentration of mortar bar at 14 days.

Table 1—Size of RVE used in micro- and macrolevel stress analysis; *h* = 12.7 mm (0.5 in.)

Aggregate size	Diameter, mm	Size of square RVE in micromodel, mm	Distance between aggregates and RVE boundary	Selected length of mortar bar, *L*, mm	Number of vertical elements in finite element mesh, n_v
No. 8	2.36	3.335	0.487	126.7	4
No. 16	1.18	1.668	0.244	126.8	8
No. 30	0.60	0.849	0.125	127.4	15
No. 50	0.30	0.426	0.063	126.9	32
No. 100	0.15	0.214	0.032	31.7	64
No. 200	0.075	0.108	0.0167	8.4	128
No. 400	0.038	0.058	0.009	4.1	256

Note: 1 mm = 0.03937 in.

model in Table 1 is determined from the volume fraction of the aggregate or the volume fraction of the cement paste given in Table 2. Figure 6(a) shows the segment *L* of the mortar bar being simulated; Fig. 6(b) shows the finite element mesh used for the stress analysis and the RVE for the micro-diffusion in one aggregate. For simplicity, the compatibility in terms of the boundary condition is not considered from Fig. 6(b) to (c) in the macro stress analysis.

Analysis procedure

Analysis was again conducted through three major steps:

- Macro-ion diffusion of alkali from the sodium hydroxide solution into the concrete is simulated by the finite difference code CDAP program; $D_{ion,macro}/B_{ion,macro}$ in Eq. (3) is taken as 1×10^{-11} m^2/s (1.55×10^{-8} in./s). For simplicity, only vertical diffusion is assumed; such an assumption is reasonable given the large aspect ratio of the specimen. The ion concentration of the solution is 0.1 (Suwito et al. 2002), and the spatial variation of the free ion concentration at 14 days is shown in Fig. 7. Finally, the spatial and temporal distribution of the free ion concentration, $C_{ion}(y,t)$, is recorded, as it will subsequently be applied as a boundary condition for the microdiffusion of ion into the individual aggregate. Note that the variation along the length of the mortar bar (x-direction) is ignored.
- Micro-coupled chemo-mechanical analysis is performed next for each of the aggregate sizes shown in Table 1. For the sake of computational efficiency, coupled micro-simulation is performed only at four equally spaced elevations in the finite element mesh (Fig. 5(a)), as opposed to at the n_v elevations shown in Table 1. Results at other elevations are simply interpolated in between. This is driven by the high computational time needed for the coupled analysis. It should be noted that such

Table 2—Material parameters used in diffusion process

Parameter	Value
Maximum time, days	14
Step size, seconds	10,000
Volume fraction of aggregate	0.65
Volume fraction of matrix	0.35
$D_{ion,micro}/B_{ion,micro}$, mm^2/s	1×10^{-10}
$\upsilon_{gel} = K_{gel}/\eta_{gel}$, mm^2/s	1×10^{-10}
Critical ion concentration C_{cr}	0.005
Constant ion concentration C_o	0.1
Volume ratio η	1.75
V_{unit}, mm^3/mm^2	0.002
Porosity of cement paste C_p, %	40

Notes: 1 mm^2/s = 0.00155 in.^{2}/s; 1 mm^3/mm^2 = 0.03937 in.^{3}/in.^{2}

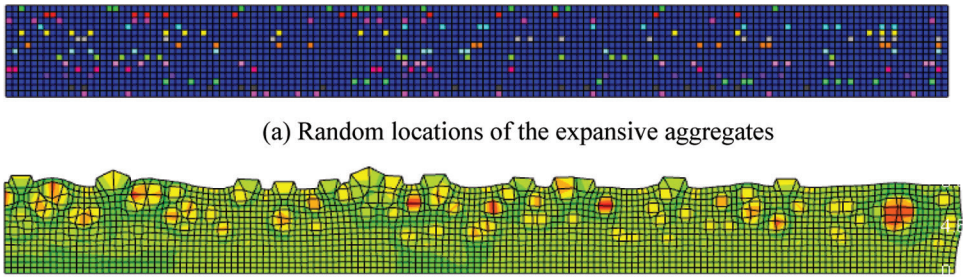

(a) Random locations of the expansive aggregates

(b) ASR induced inhomogeneous macro deformation

Fig. 8—Macro finite element stress analysis.

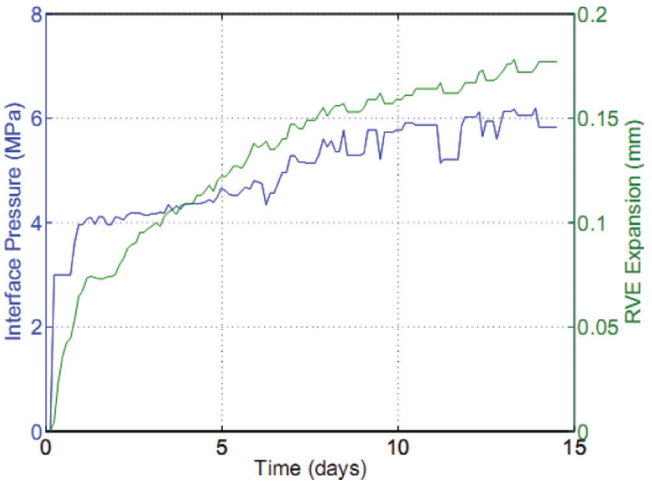

Fig. 9—Pressure and expansion versus time.

an analysis will yield a coefficient of expansion at predefined elevations and at a given time. The procedure is as follows:

- Subdivide the mortar bar RVE into four layers and determine the ion concentration histogram at that level from the preliminary macrodiffusion analysis (Fig. 5(a)). This free ion concentration will constitute the ion boundary condition at the aggregate surface in the micro-ion diffusion analysis.
- Perform the coupled chemo-mechanical analysis of the selected RVE in each layer (Fig. 5(c)). The selected parameters used in the micro-ion diffusion analyses (Suwito et al. 2002) and the parameters used in the stress analysis are shown in Tables 2 and 3, respectively. It should be noted that in the MERLIN analysis, interface elements were used around each particle and a nonlinear continuum element was used for the concrete, thus allowing for the formation of either smeared cracks or crushing of the concrete. This is another new development compared to the analytical solution used in Suwito et al. (2002). No attempt is made to reconcile the compatibility of displacements (or tractions) between the analysis of the RVE (Fig. 5(c)) and the displacements in the macro-analysis (Fig. 6(b)).
- Compute the expansion coefficient due to ASR gel of the selected RVE after 14 days for each of the four layers.
- Through a regression analysis, determine an equation that characterizes the ASR expansion coefficient in terms of distance from the top of the mortar bar.

- Macro stress analysis: It is assumed that only 10% of the aggregates are reactive. These are first randomly located in the finite element mesh and then assigned a pseudo-thermal expansion governed by the previously obtained linear regression (Fig. 8(a)). A linear elastic finite element analysis of the entire mortar bar model is then performed (it was determined that a nonlinear model was unnecessary, as no major cracks were formed) and the ASR-induced expansion is determined from the point of maximum displacement (Fig. 8(b)).

Investigation results

First, an example of ASR investigation in the mortar bar using 10% of the No. 30 (0.6 mm) reactive aggregate is shown. In the microlevel analysis, only the results of the RVE at the top layer of the mortar bar are shown. Figure 9 shows the development of the interface pressure around the reactive aggregate with time up to 14 days.

At first, the rate of gel formation is faster than the diffusion capability of gel into the cement paste around the aggregate; thus, there is a gradual buildup of pressure around the aggregate. Once this pressure reaches the tensile strength of the cement paste (3.0 MPa [435.1 psi]), microcracks form, releasing the pressure increase by allowing further diffusion of the gel. Because the rate of gel formation is still faster than the rate of gel diffusion into the cement paste around the aggregate, the pressure can then be greater than the tensile strength of the cement paste. This is illustrated by Fig. 9.

The ASR expansion starts immediately when the gel fills the porous zone around the aggregate and then permeates into interconnected pores in the cement paste matrix (Sellier et al. 1995). After the ASR expansion around the aggregates starts, it results in the reaction force at the support and the displacement of the RVE, which increase gradually with time in the x-direction. After $t = 0.2$ days, ASR expansion results in no further change in the reaction at the support but the displacement of the RVE still increases with time. This may be due to the strain-softening behavior of concrete. After the strain softening occurs, the reaction at the support in the x-direction remains constant, while the RVE strain keeps increasing.

After investigating the coefficient of expansion due to ASR gel on the No. 30 (0.6 mm) reactive RVE of the top element in all four layers considered (as shown in Fig. 5(a)) at 14 days, the expansion coefficients of those four points are plotted into the graph along the depth from the top of the bar

Table 3—Material parameters used in stress analysis

Parameter	Value	
	Cement paste	Aggregate
Element group	Fracture plastic model	Isotropic linear elastic
Modulus of elasticity, N/mm^2	1.2×10^4	8×10^4
Poisson's ratio	0.2	0.2
Uniaxial tensile strength, N/mm^2	3.0	—
Fracture energy, N/mm	7.0×10^{-2}	—
Uniaxial compressive strength, N/mm^2	–30.0	—
Return direction factor	0	—
Compressive critical displacement, mm	–0.5	—
Failure surface roundness factor	5.5×10^{-1}	—
Onset of compression nonlinearity, N/mm^2	–15.0	—
Plastic strain at f_c'	-8×10^{-4}	—

Notes: 1 N/mm^2 = 145.0377 lb/in.^{2}; 1 N/mm = 5.7102 lb/in.; 1 mm = 0.03937 in.

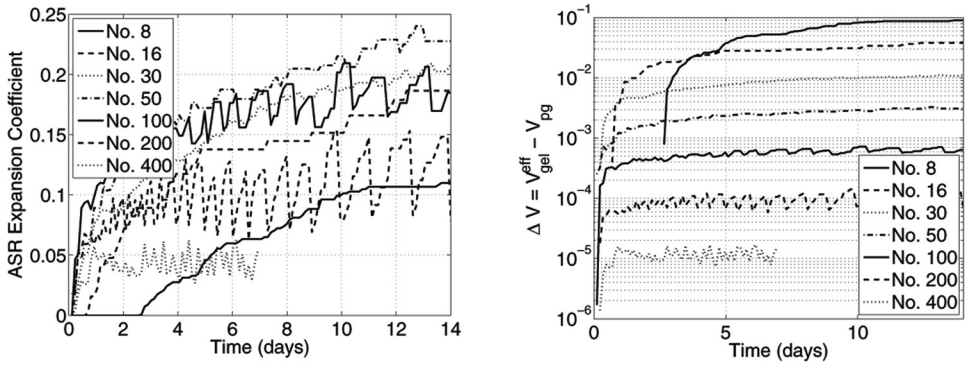

(a) Simulated coefficients of ASR expansion with time in terms of aggregate sizes

(b) Temporal variation of non-absorbed gel volume

Fig. 10—Simulation results for all aggregates.

and the equation of the expansion coefficient is determined, as shown in Fig. 5(b).

In the macrolevel, the random locations of RVE of the 10% No. 30 (0.6 mm) reactive aggregate inside the mortar bar are shown in Fig. 8(a). The inhomogeneous macro deformation (Fig. 8(b)) will induce an anisotropic deformation.

The expansion coefficient of each aggregate size with respect to time is shown in Fig. 10(a). This figure reveals an unanticipated oscillation for aggregates of size 100 or smaller. This can be explained by revisiting Eq. (15), from which the ASR expansion coefficient is determined and which is linearly dependent on the volume of nonabsorbed gel. However, the ion diffusion and the gel formation (for the reactive aggregates) depend on the size of the aggregate itself. On the other hand, gel diffusion depends on the distance between the aggregates and boundary of the RVE, which are listed in Table 1. The interface pressure between the aggregate and the cement paste increases when the rate of gel formation is greater than the rate of gel diffusion. On the other hand, the pressure drops when the rate of gel diffusion is greater than the rate of gel formation. Therefore, for small aggregate sizes, the gel formation can result in large interface pressure (high gel concentration at the boundary of the aggregate) at the first time step; then, it causes an increased gel diffusion rate and the interface pressure drops in the next time step. Figure 10(b) shows the temporal variation of nonabsorbed gel volume; oscillation begins for aggregates of size 100 and smaller.

Now, this study focuses on the expansion curves for aggregate sizes No. 8 (0.84 mm). Larive (1998) presented the following kinetic equation as the one governing ASR expansion

$$\xi(t,\theta) = \varepsilon_{ASR}^{\infty} \frac{1 - e^{-\frac{t}{\tau_C(\theta)}}}{1 + e^{-\frac{(t-\tau_L(\theta))}{\tau_C(\theta)}}} \tag{18}$$

in terms of the maximum expansion $\varepsilon^{\infty}_{ASR}$ and two temporal parameters: latency time τ_L and characteristic time τ_C (Fig. 11). Through proper adjustment of these three parameters, practically any expansion can be reproduced, including cases where the reaction does not stop. It recognizes the thermodynamical nature of the reaction through an Arthmus-like equation, where θ is the actual absolute temperature and θ_0 is the absolute temperature corresponding to τ_L and τ_C. Because the experimental tests, as reported by Jin et al. (2000), were conducted at 80°C (176°F) for 14 days, Eq. (18)

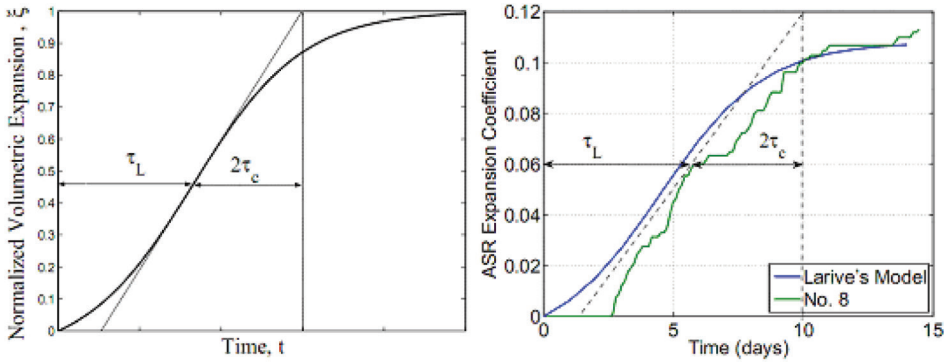

(a) Kinetic model of an ASR Expansion (Larive, 1998) (b) Kinetics of Aggregate sizes No. 8

Fig. 11—Kinetics of ASR expansion.

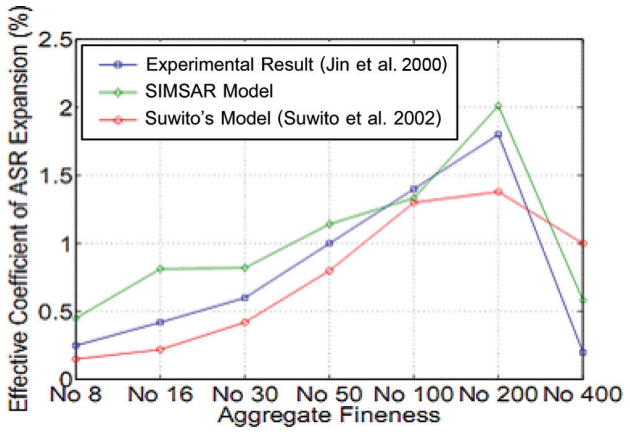

Fig. 12—Expansion versus fineness.

is superimposed on the model prediction with $\varepsilon^{\infty}_{ASR}$, τ_L, and τ_C corresponding to 0.108, 4.5 days, and 2 days, respectively. Figure 11(b) shows the superposition of the curve-fitted model of Larive (1998) to match the expansion kinetic obtained from the presented numerical model. An adequate correlation being obtained with reasonable parameters, it is concluded that through proper refinements of the numerical model, the kinetic of the ASR expansion can be obtained and used for the macro-analysis of massive structures, such as dams (Saouma et al. 2007).

One can then apply the procedure described in conjunction with Fig. 5(b) through a finite element analysis. Figure 8(b) shows the deformed shape, which is irregular due to the random distribution of the reactive aggregates.

Finally, the numerically simulated ASR expansions of the seven aggregate sizes are compared with the experimental results and the numerical model obtained from Suwito et al. (2002) in Fig. 12 after 14 days. Note the close similarity between the experimentally obtained results and those obtained through the proposed numerical simulation.

CONCLUSIONS

The ASR micromodel developed by Suwito et al. (2002) is modified and implemented into a numerical (C++) code. The model involves two diffusion equations and the stress analysis due to the ASR gel. The numerical model handles the two diffusion phenomenon through a finite difference analysis and couples with an existing finite element code (MERLIN) to account for the coupling between the diffusion processes and the stress analysis.

There are several new developments in this model. The ion diffusion parameter is now dependent on the ion concentration. The ASR expansion ratio is dependent on the internal relative humidity. The finite difference and finite element schemes allow more complicated geometries for both aggregate and specimens, and the numerical method also allow anisotropic deformation induced by ASR. More importantly, the use of MERLIN in the coupled analysis can handle the strain softening of cement paste induced by ASR, while the analytical solution of Suwito et al. (2002) was based on linear elastic analysis.

The numerical results of ASR expansion in mortar bars obtained from the macro and micro numerical analysis mentioned in this study are then compared with available experimental results and the results obtained from the study of Suwito et al. (2002). The strains of the RVE of the mortar bar obtained in this study are quite close to the strains obtained from both the experimental results and the study of Suwito et al. (2002). Also, the interface pressure generated by the gel around the aggregate obtained from coupled SIMSAR-MERLIN in the microlevel analysis is more realistic—specifically, the pressure is not too high such as the one obtained from Suwito et al. (2002) because the finite element code used to perform the stress analysis can handle the softening behavior of concrete. Finally, the kinetics of the expansion compared favorably well with the model of Larive (1998), thus providing a transition model from micromodeling to macromodeling of ASR expansion.

ACKNOWLEDGMENTS

The authors would like to thank Y. P. Xi, who reviewed earlier versions of the manuscript and clarified some key issues pertaining to the model of Suwito, for his support. The first author would also like to acknowledge the support of the Department of Civil Engineering, Faculty of Engineering, Ubon Ratchathani University, Thailand.

NOTATION

B_{ion}	=	binding capacity of aggregate
$B_{ion,macro}$	=	binding capacity of concrete
C_{cr}	=	critical concentration of ion, %
C_{gel}	=	gel concentration, %
C_{ion}	=	ion concentration, %
C_o	=	ion constant concentration at boundary of aggregate, %
C_p	=	porosity of cement paste, %
D_{ion}	=	ion permeability of aggregate
$D_{ion,macro}$	=	ion permeability of concrete
f_t'	=	tensile strength of concrete, MPa
H	=	pore relative humidity, %

K_{gel}	=	gel permeability of porous cement paste
P_{int}	=	interface pressure caused by gel formation around aggregate, MPa
t	=	time, seconds
V_{R_i}	=	volume of reacted aggregate of size R_i, mm^3
$V_a^{R_i}$	=	volume of aggregate with size R_i, mm^3
$V_{gel}^{R_i}$	=	volume of ASR gel created at boundary of aggregate size R_i, mm^3
$V_{pg}^{R_i}$	=	gel volume in porous cement surrounding aggregate with size R_i, mm^3
$V_{pore}^{R_i}$	=	volume of ITZ around reacted aggregate, mm^3
α_{eff}	=	volumetric average of ASR expansions of concrete
$\alpha_i^{R_i}$	=	expansion coefficient due to gel formation around aggregate with size R_i
β	=	state function for cement paste
ϕ_i	=	volumetric fraction of aggregate size R_i
η	=	volume ratio of ASR gel to reacted aggregate
η_{gel}	=	viscosity of gel

REFERENCES

Červenka, J., and Papanikolaou, V. K., 2008, "Three Dimensional Combined Fracture-Plastic Material Model for Concrete," *International Journal of Plasticity*, V. 24, No. 12, pp. 2192-2220.

Dunant, C., and Scrivener, K., 2010, "Micro-Mechanical Modelling of Alkali-Silica-Reaction-Induced Degradation Using the Amie Framework," *Cement and Concrete Research*, V. 40, No. 4, Apr., pp. 517-525.

Glasser, D., and Kataoka, N., 1981, "The Chemistry of Alkali-Aggregate Reaction," *Cement and Concrete Research*, V. 11, No. 1, pp. 1-9.

Jin, W.; Meyer, C.; and Baxter, S., 2000, "'Glascrete'—Concrete with Glass Aggregate," *ACI Materials Journal*, V. 97, No. 2, Mar.-Apr., pp. 208-213.

Larive, C., 1998, "Apports Combinés de l'Experimentation et de la Modélisation à la Comprehension del' Alcali-Réaction et de ses Effets Mécaniques," PhD thesis, Thése de Doctorat, Laboratoire Central des Ponts et Chaussées, Paris, France, 396 pp. (in French)

Multon, S.; Sellier, A.; and Cyr, M., 2009, "Chemo-Mechanical Modeling for Prediction of Alkali Silica Reaction (ASR) Expansion," *Cement and Concrete Research*, V. 39, No. 6, June, pp. 490-500.

Poyet, S.; Sellier, A.; Capra, B.; Foray, G.; Torrenti, J.; Cognon, H.; and Bourdarot, E., 2007, "Chemical Modelling of Alkali Silica Reaction: Influence of the Reactive Aggregate Size Distribution," *Materials and Structures*, V. 40, No. 2, pp. 229-239.

Puatatsananon, W., 2002, "Deterioration of Reinforced and Massive Concrete: A Multi-Physics Approach," PhD thesis, University of Colorado, Boulder, Boulder, CO.

Saouma, V.; Červenka, J.; and Reich, R., 2010, "MERLIN Finite Element User's Manual," http://civil.colorado.edu/~saouma/pdf/users.pdf. (last accessed Nov. 25, 2012)

Saouma, V.; Perotti, L.; and Shimpo, T., 2007, "Stress Analysis of Concrete Structures Subjected to Alkali-Aggregate Reactions," *ACI Materials Journal*, V. 104, No. 5, Sept.-Oct., pp. 532-541.

Sellier, A.; Bournazel, J. P.; and Mebarki, A., 1995, "Une Modelisation de la Reaction Alcalis-Granulat Integrant une Description des Phenomenes Aleatoires Locaux," *Materials and Structures*, V. 28, pp. 373-383. (in French)

Stanton, T., 1940, "Expansion of Concrete through Reaction between Cement and Aggregate," *Proceedings of ASCE*, V. 66, pp. 1781-1811.

Suwito, A.; Jin, W.; Meyer, C.; and Xi, Y., 1998, "Theoretical Modeling on Expansion and Damage due to Alkali-Silica Reaction," *Proceedings of 12th Engineering Mechanics Conference*, San Diego, CA, pp. 1175-1178.

Suwito, A.; Jin, W.; Xi, Y.; and Meyer, C., 2002, "A Mathematical Model for the Pessimum Effect of ASR in Concrete," *Concrete Science and Engineering*, V. 4, No. 13, pp. 23-34.

Swamy, R., ed., 1992, *The Alkali-Silica Reaction in Concrete*, Van Nostrand Reinhold, New York, pp. 1-28.

Ulm, F.; Coussy, O.; Kefei, L.; and Larive, C., 2000, "Thermo-Chemo-Mechanics of ASR Expansion in Concrete Structures," *Journal of Engineering Mechanics*, ASCE, V. 126, No. 3, Mar., pp. 233-242.